Advances in Recirculating Superconducting Proton Linac Study

Ji Qiang

Accelerator Modeling Program
Lawrence Berkeley National Laboratory

MSU/FRIB
Accelerator Physics/Engineering Seminars
September 24, 2021

Outline

- Introduction
- Multi-GeV recirculating superconducting proton linac
- Beam dynamics design/simulation of a double pass proton linac
- Effects of overtaking collision in the CW double pass proton linac
- Phase shifters for a multi-pass proton linac
- Future work

High Power GeV Superconducting Proton Linac Can Have Many Applications in Science and Industry

- Accelerator driven tritium production
- Driver for spallation neutron sources
- Driver for high energy physics studies
- Accelerator driven nuclear energy production
- …

Accelerator Driven Spallation Neutron Sources

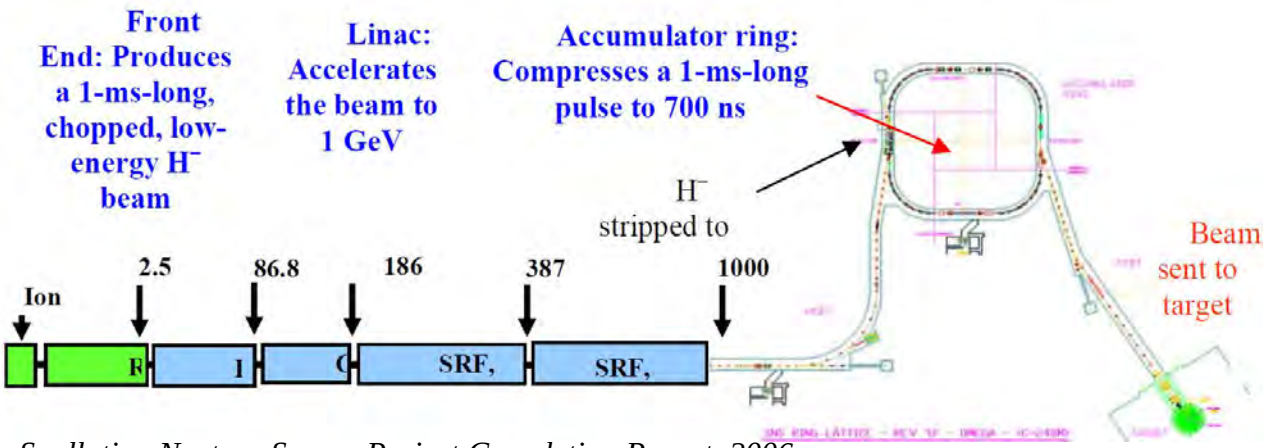

Spallation Neutron Source Project Completion Report, 2006.

Baseline parameters for the SNS accelerator		
Kinetic energy	GeV	1.0
Beam power on target	MW	1.4
Average current on target	mA	1.4
Linac beam macropulse duty factor	%	6
Average macropulse H⁻ current	mA	26
Peak linac current	mA	38
Linac average beam current	mA	1.6
SRF cryomodule number		11 + 12
SRF cavity number		33 + 48
Peak gradient medium beta	MV/m	27.5
Peak gradient high beta	MV/m	35

Table 1: ESS Main Parameters

Parameter	2012 Baseline	2013 Baseline
Ion species	Proton	Proton
Energy [GeV]	2.5	2.0
Beam power [MW]	5	5
Repetition rate [Hz]	14	14
Beam current [mA]	50	62.5
Beam pulse [ms]	2.86	2.86
Duty cycle [%]	4	4

M. Eshraqi et al., 2014.

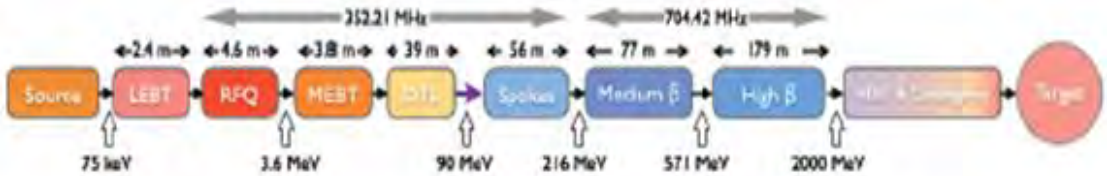

Figure 1: Block layout of the ESS baseline linac 2013, OptimusPlus (not to scale). Warm colored boxes represent the normal conducting components and cold color boxes the superconducting sections.

Accelerator Driver for High Energy Physics Applications

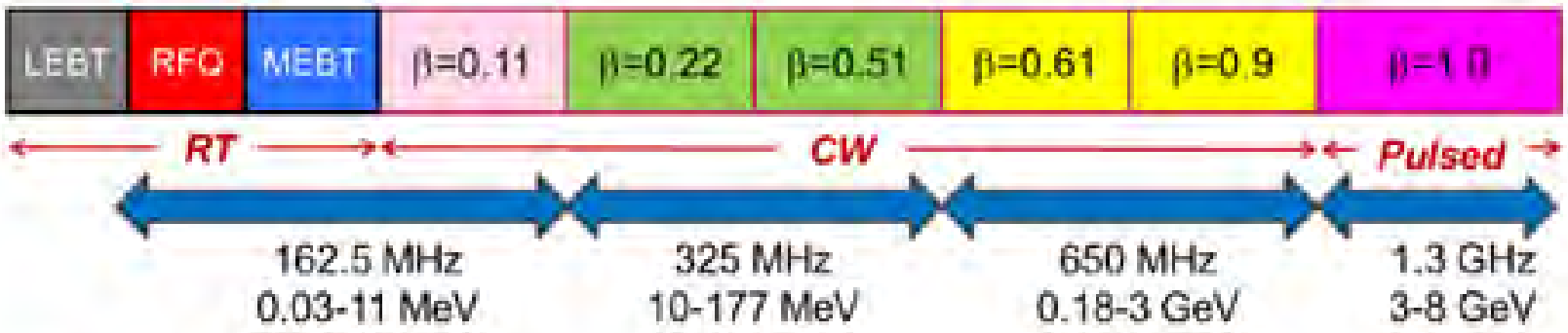

Figure III-1: The Project X Linacs

S. Holmes, et al., Project X Reference Design Report, Project X-document 776-v7, 2013.

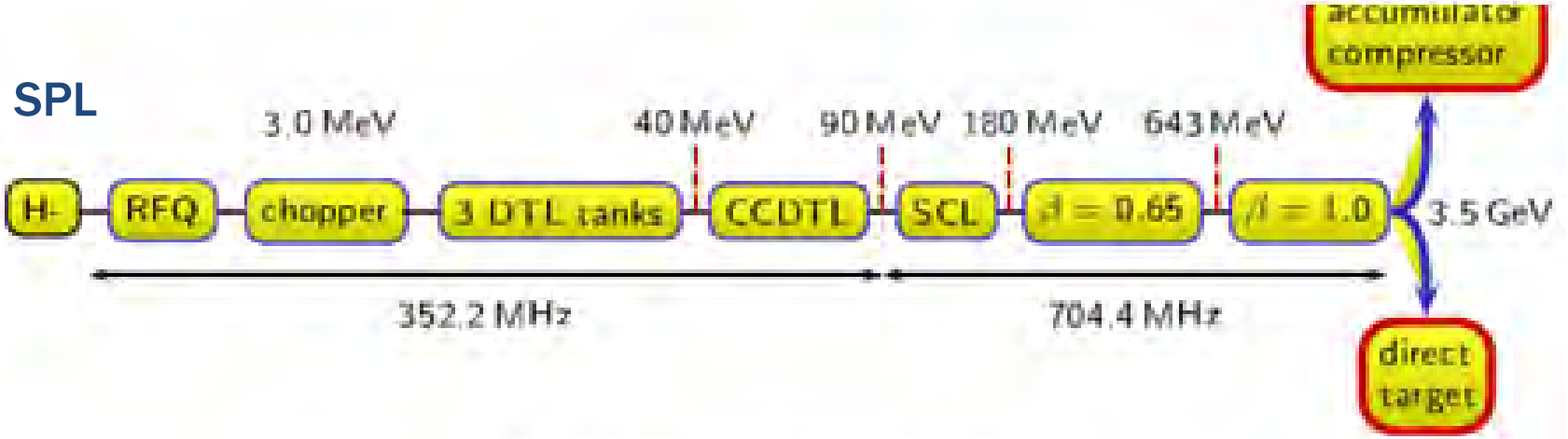

Fig. 2.3: Schematic layout of the linac

F. Gerigk, et al., Conceptual Design of the SPL II, CERN-2006-006, 2006.

Accelerator Driven System for Nuclear Energy Production

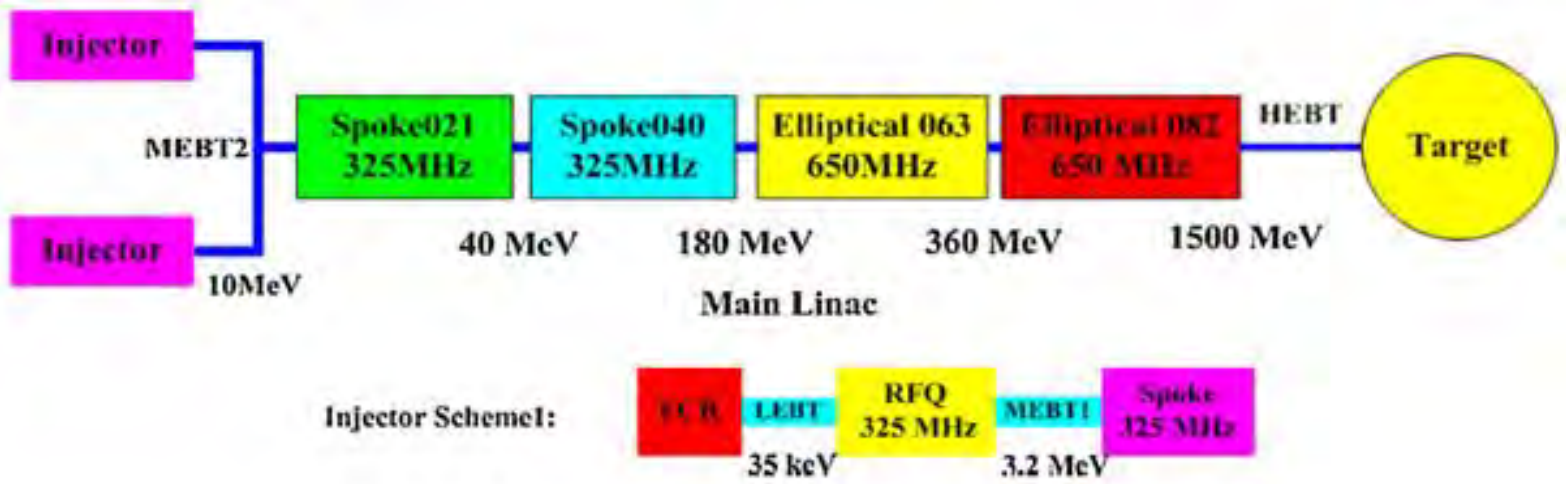

Z. Li, et al., Physical Review ST Accelerators and Beams 16 (2013) 080101.

FIG. 3. Layout of the C-ADS driver accelerators.

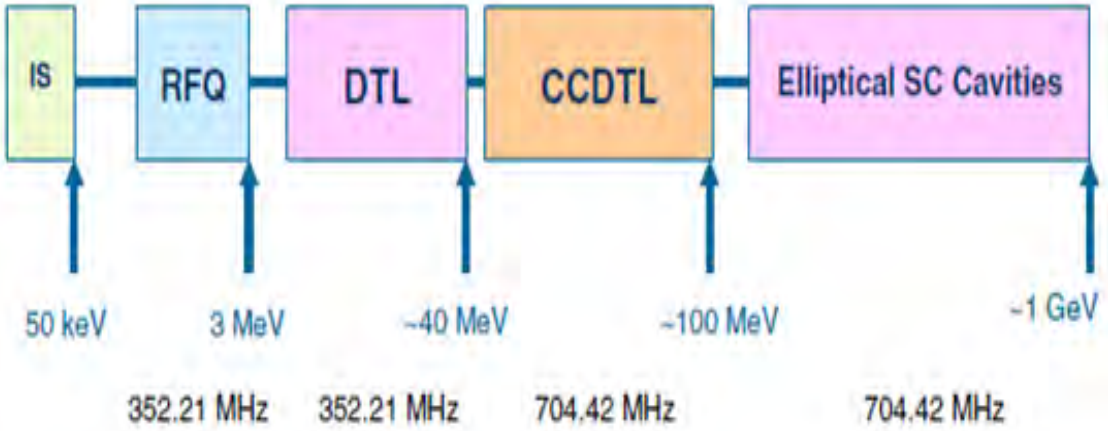

Figure 1. Lay-out of the 1 GeV Linac.

R. Pande,etal.,Pramana—Journal ofPhysics78(2012)247.

But Superconducting Proton Linac is Expensive…

Linac vs. RCS Revisited

PIP-III

"

- Project X was a fairly mature, linac-based proposal that would produce high power at 60-120 GeV, while supporting a broad program at lower energies
  - It was judged to be too expensive.
- The current charge is to find the most cost effective way to *achieve the physics goals of DUNE*
  - Currently no explicit mandate for a low energy program
- Unless there's a huge breakthrough in SRF technology, an RCS is the best way to do this, HOWEVER
- The charge says the final recommendation "may include alternatives"
  - The alternative will almost certainly be a linac-based option.
  - Reduced costs and/or changing physics priorities may well make that the ultimate frontrunner.

"

- Eric Prebys at 2015 Fermilab workshop

A Potential Lower Cost Solution: Recirculating Proton Linac

Recirculating Electron Linac has been built and under operation (e.g. JLAB Recirculating Electron Linac)

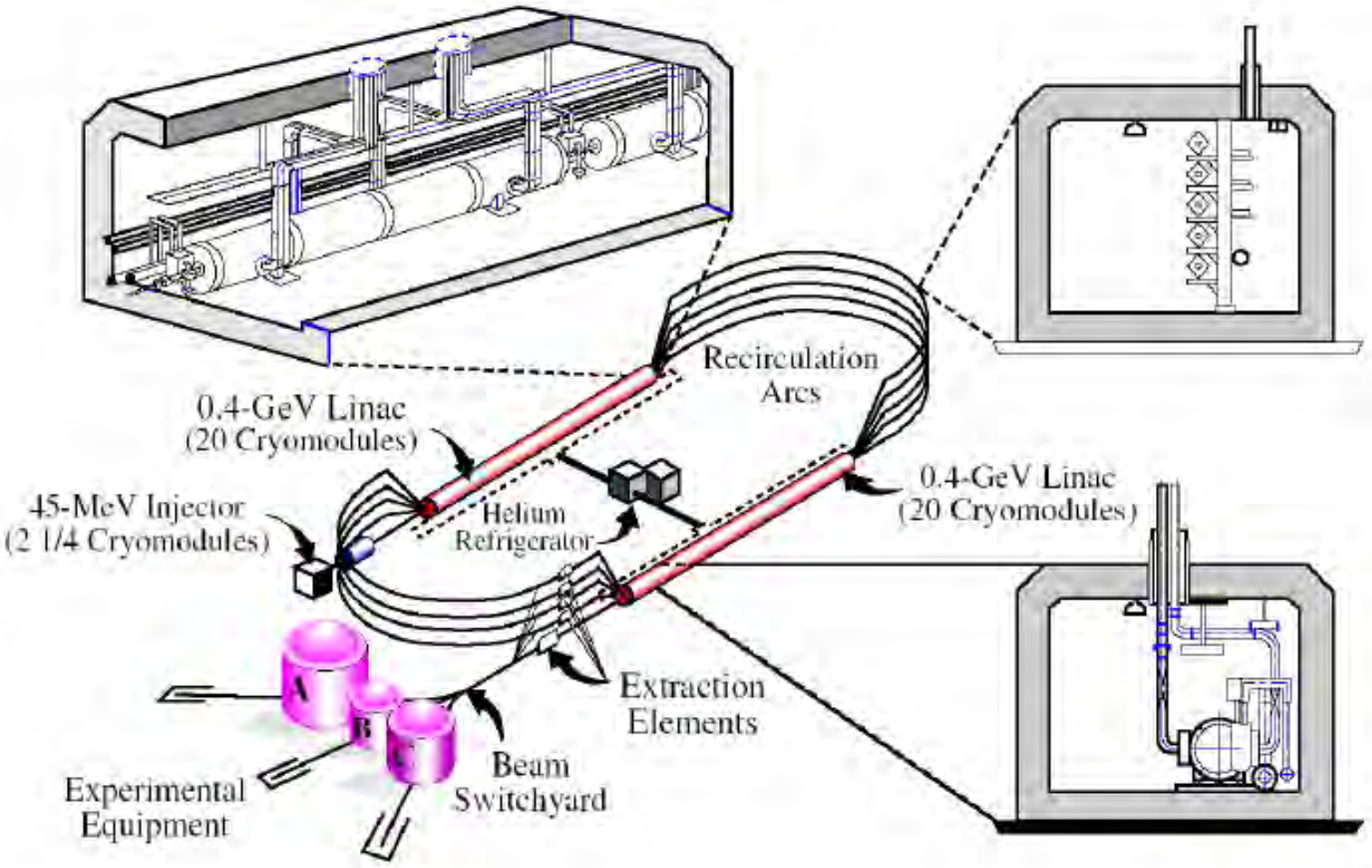

But there is no recirculating proton linac in the world…

Significant Differences between Proton Linac and Electron Linac

- **Electron velocity approaches to speed of light over a few MeVs**
- **Acceleration efficiency (transit time factor) independent of energy**
- **Typical electron linac consists of a single type of RF cavity (C band or S band or SC or …)**

- Proton velocity varies during the process of acceleration up to GeVs
- Acceleration efficiency depends on the proton energy
- Typical proton linac consists of many type of RF cavities with different geometries (DTL, CCL, CCDTL, SC,…)

recirculating linac uses a single type of RF cavity for multiple energy beam

A Reasonable Proton Energy Bandwidth Can Be Achieved with Appropriate Choice of RF Cavity Structure

$$\Delta E_c = qVT\cos(\phi)$$

$$T_0(\beta) = \frac{2\beta}{\pi n}\left(\frac{\sin(\pi n(\beta-\beta_G)/(2\beta))}{\beta-\beta_G} - (-1)^n\frac{\sin(\pi n(\beta+\beta_G)/(2\beta))}{\beta+\beta_G}\right)$$

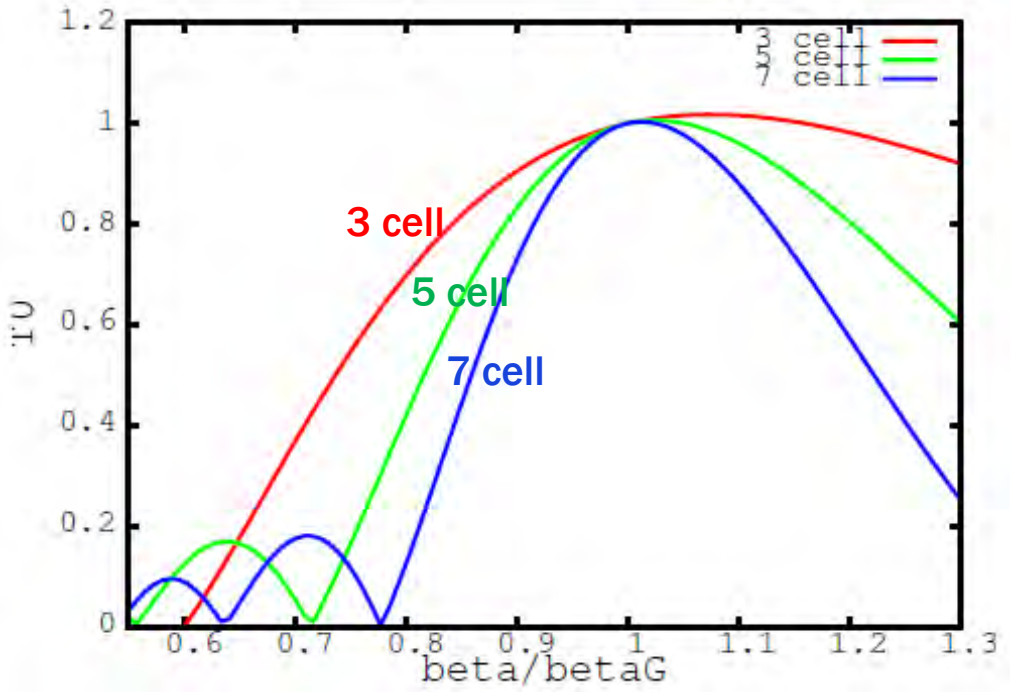

- A single type of cavity can cover a range of proton energy with appropriate cell numbers
- A multi-GeV recirculating proton linac could be realized with multiple energy sections

A Multi-Section Multi-GeV Recirculating Proton Linac (~a factor of 5 reduction of superconducting cavities)

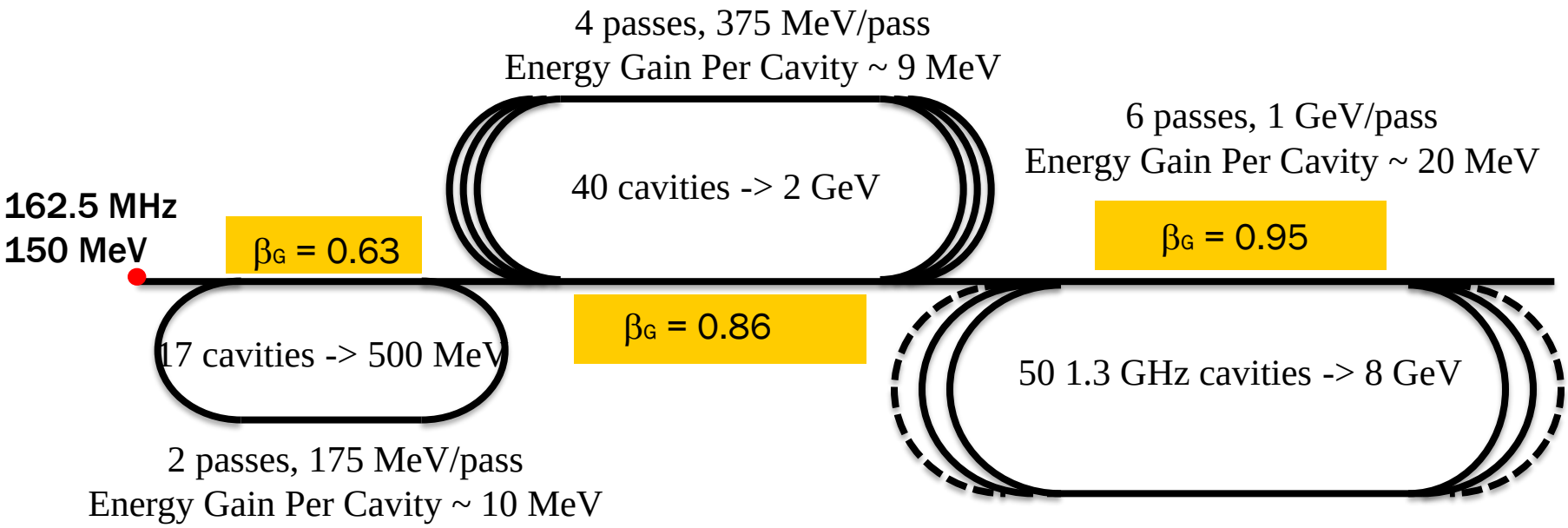

- Total number of superconducting cavities: 494 -> 107
- Shorten the distance of straight accelerating section

Fermilab 650 MHz 5 cell superconducting cavity (CW): $E_{acc} \geq 15 MV/m$

J. Qiang, Nuclear Instruments & Methods in Physics Research A 795, p. 77 (2015).

Relative RF Acceleration Phase Changes in Multiple Beam Passes

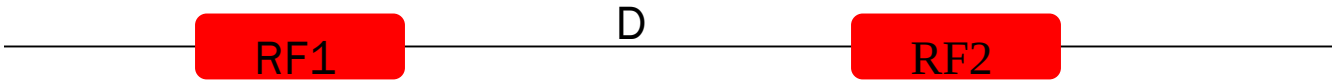

$$\Delta E_1 = V_1 T_1 \cos(\omega t + \phi_1) \qquad \Delta E_2 = V_2 T_2 \cos(\omega t + \phi_2)$$

Phase slippage with proton energy:

$$\delta\phi = \omega \frac{D}{V}$$

D ⟶ distance between RF1 and RF2

V ⟶ proton velocity after RF1

Possible solutions:

- Fast adjustment of RF cavity driven phase versus energy
- Fast adjustment of RF cavity frequency versus energy

- Use of synchronous acceleration condition:

$$t_i^m - t_i^n = \pm k T_{rf}, \quad k = 0, 1, 2, 3, \cdots$$

Synchronous Condition Can be Met with Variable Separation of Cavities in the Two Pass Section

No need to adjust RF cavity phase/frequency during the two pass acceleration

Proton Kinetic Energy vs. Distance

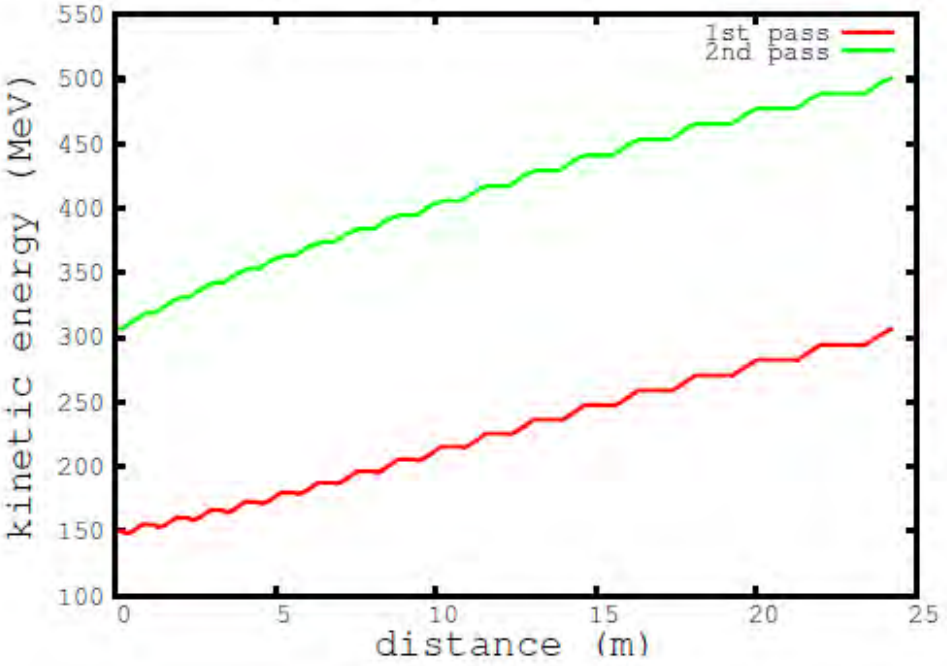

Separation Distance vs. Cavity Number

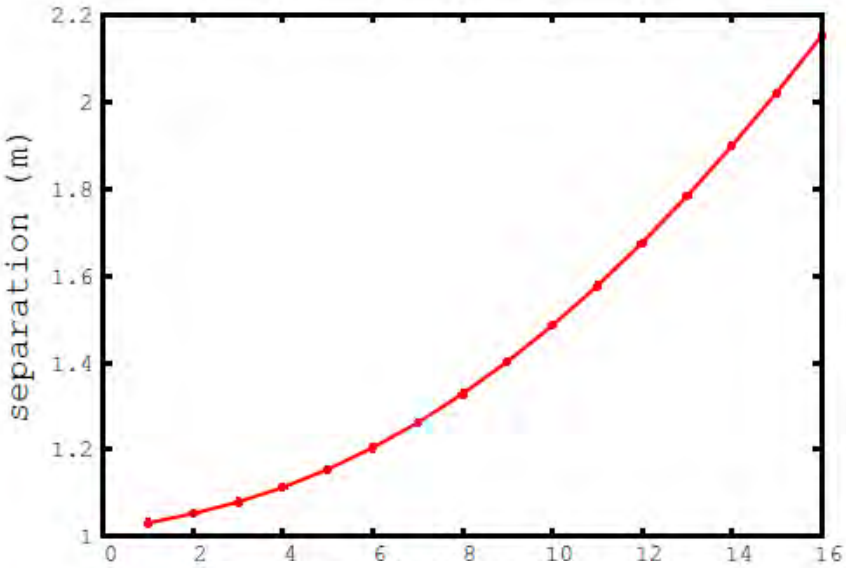

Beam Dynamics Design/Simulation of the Double Pass Section

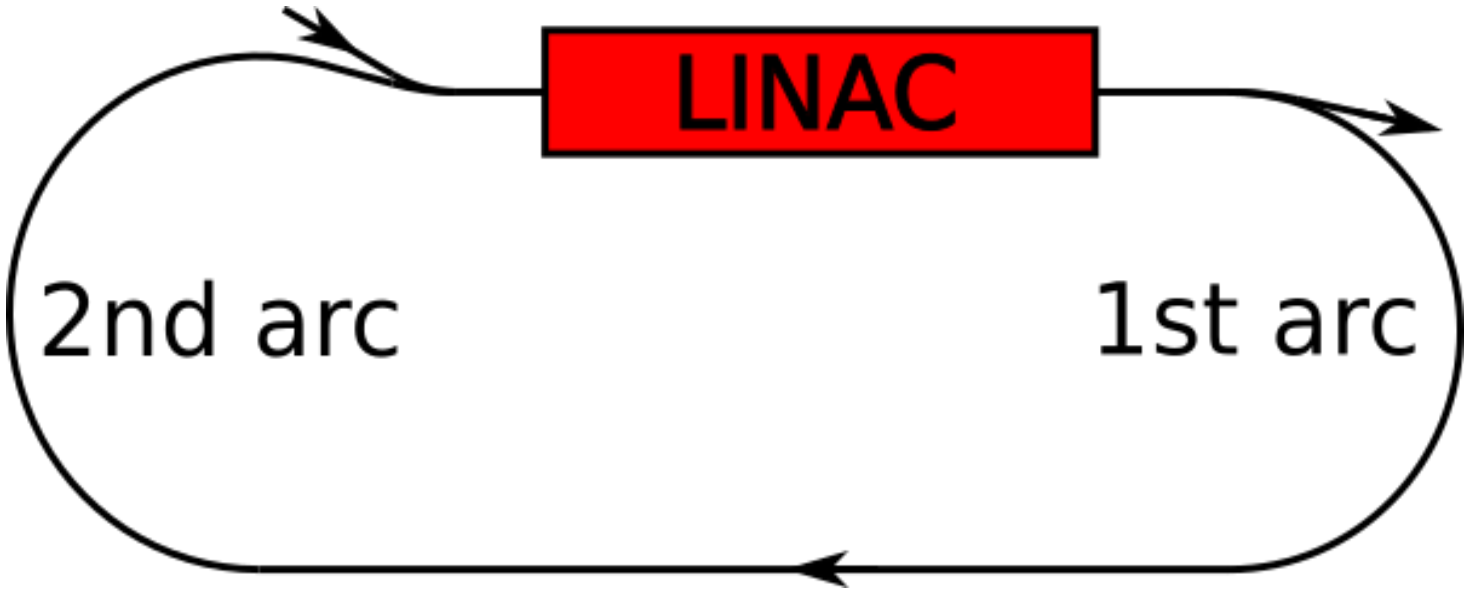

K. Hwang and J. Qiang, Phys. Rev. Accel. Beams 20, 040401 (2017).

Non-Periodic Lattice Design by Optimizing the Envelope Oscilation and Emittance Growth w.r.p Quadrupole Settings

- Alternative phase focusing is used to enhance the transverse focusing for the 1st four cavities
- Integrate the Differential Evolution optimizer with self-consistent beam-dynamics simulation using the IMPACT(Z) code.
- Maintain smooth envelope oscillation evolution.
- Control emittance growth.

$$\begin{aligned} \text{cost} &= w_\sigma \sum_{i=0}^{N} \sum_{j=x,y} \left(\sigma_j(i) - \sigma\right)^{p_\sigma} \\ &\quad + w_\epsilon \sum_{j=x,y,z} \left(\epsilon_j(L) - \epsilon_j(0)\right)^{p_\epsilon} \end{aligned}$$

Reasonable Transverse RMS Sizes and Emittances Evolution through the Double Pass Proton Linac from Simulation (40 mA)

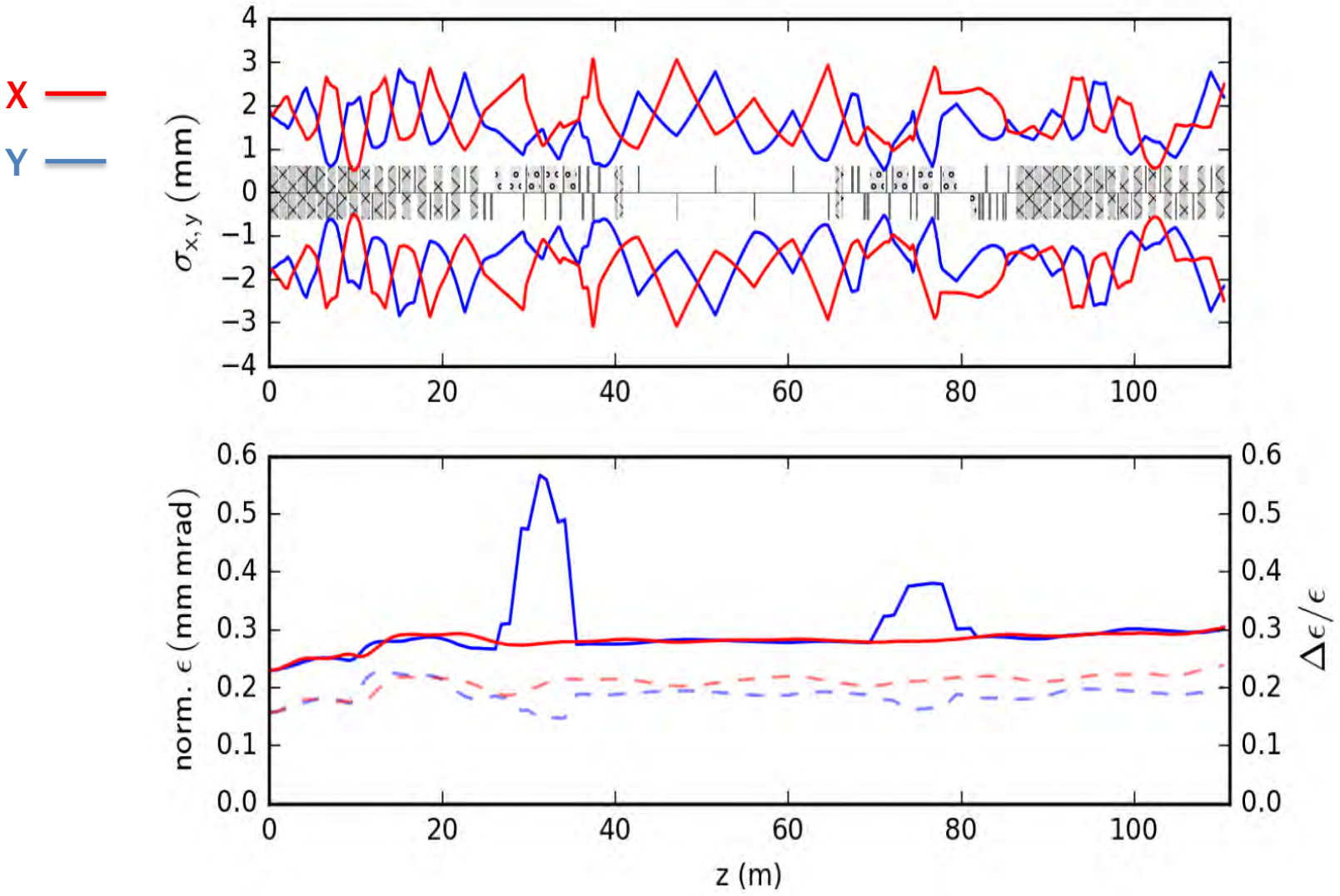

Reasonable Longitudinal RMS Size and Emittance Evolution through the Double Pass Proton Linac from Simulation (40mA)

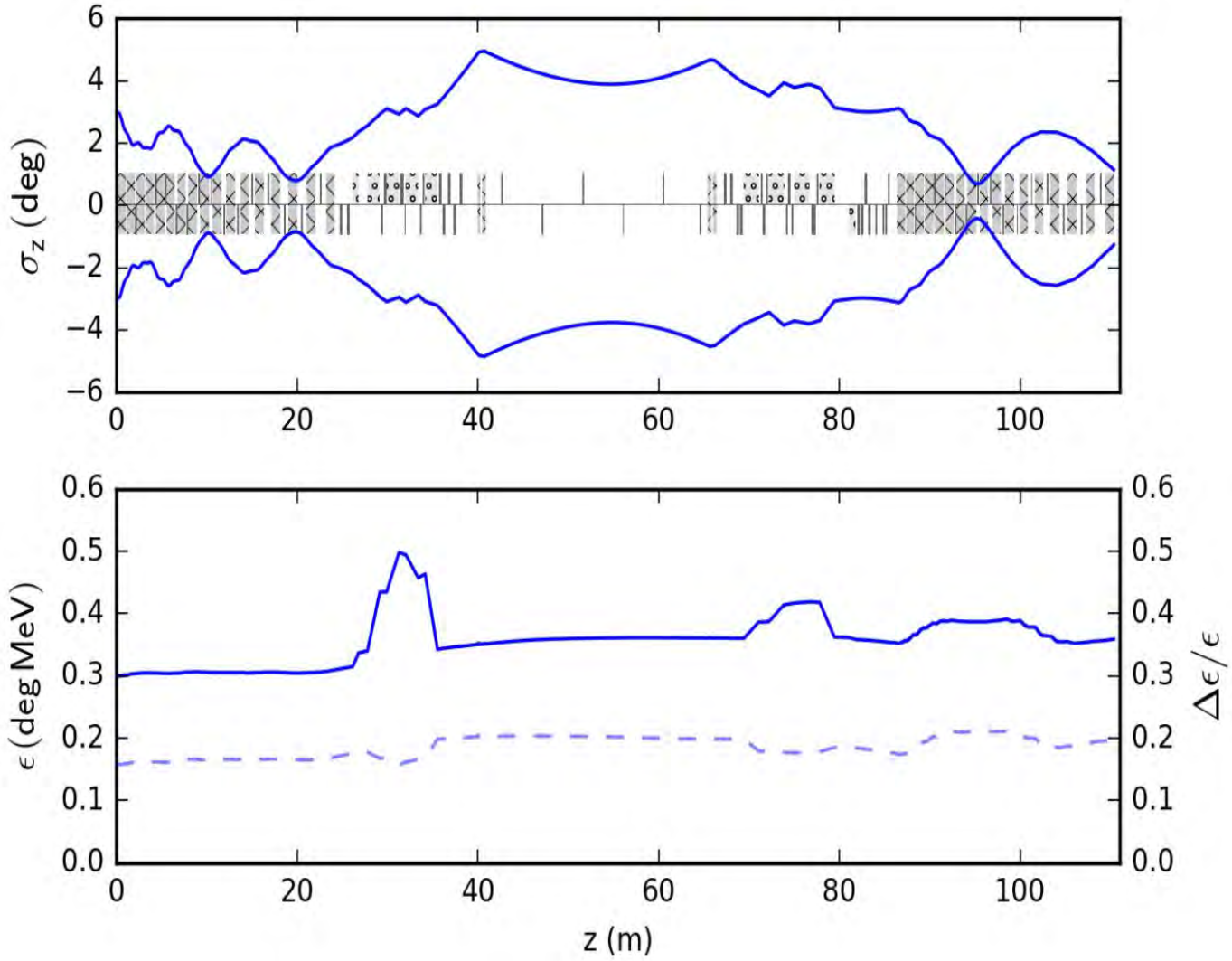

Effects of Overtaking Collision in CW Double Pass Proton Linac

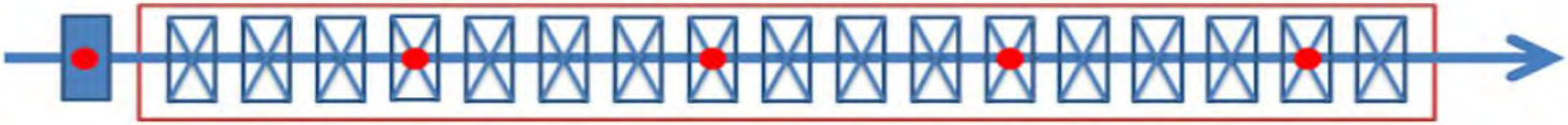

Injector frequency 162.5 MHz, SC frequency 650 MHz, 10 collisions

Drift Cavity Collision Point

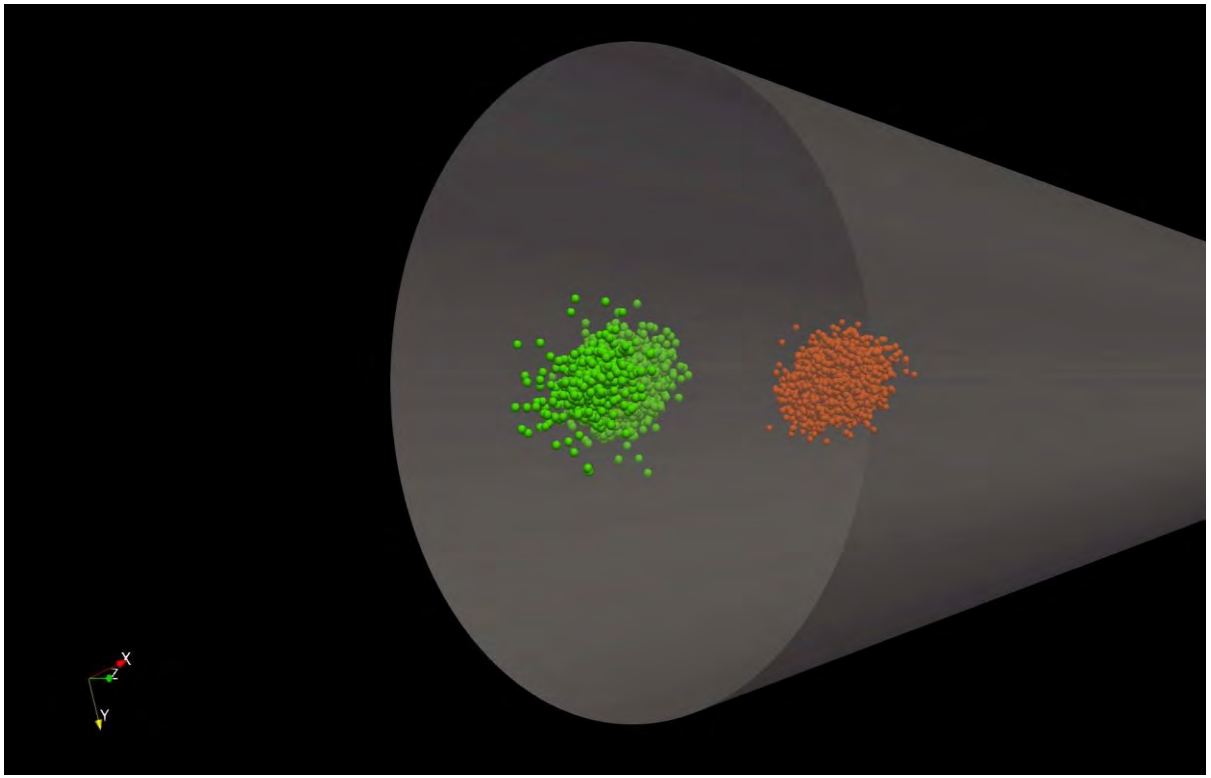

Y. Tao, J. Qiang, K. Hwang, linac, Phys. Rev. Accel. Beams 20, 124202 (2017).

RMS Sizes Evolution w/o Collision through the Double Pass Linac

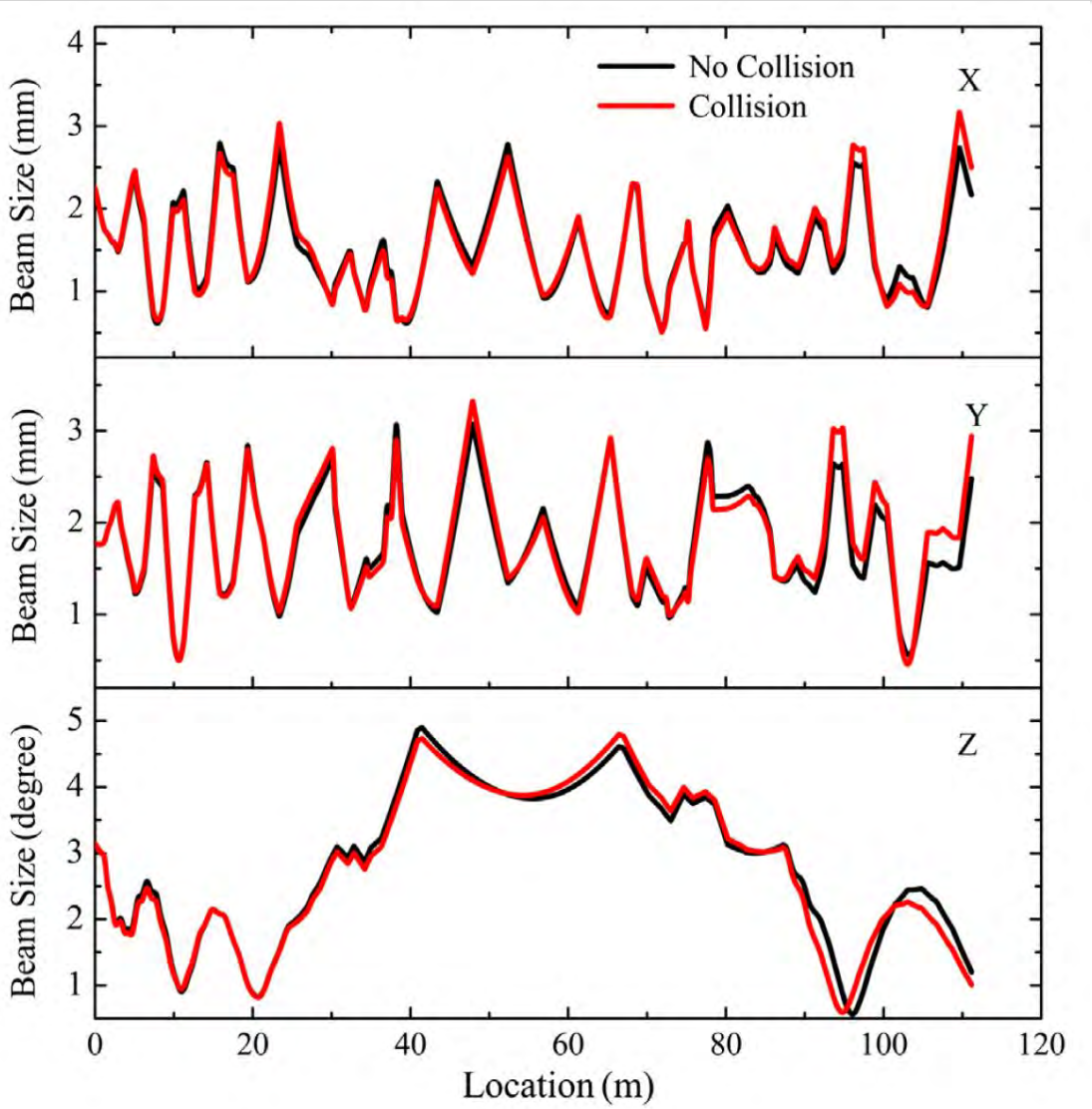

RMS Emittances Evolution w/o Collision through the Double Pass Linac

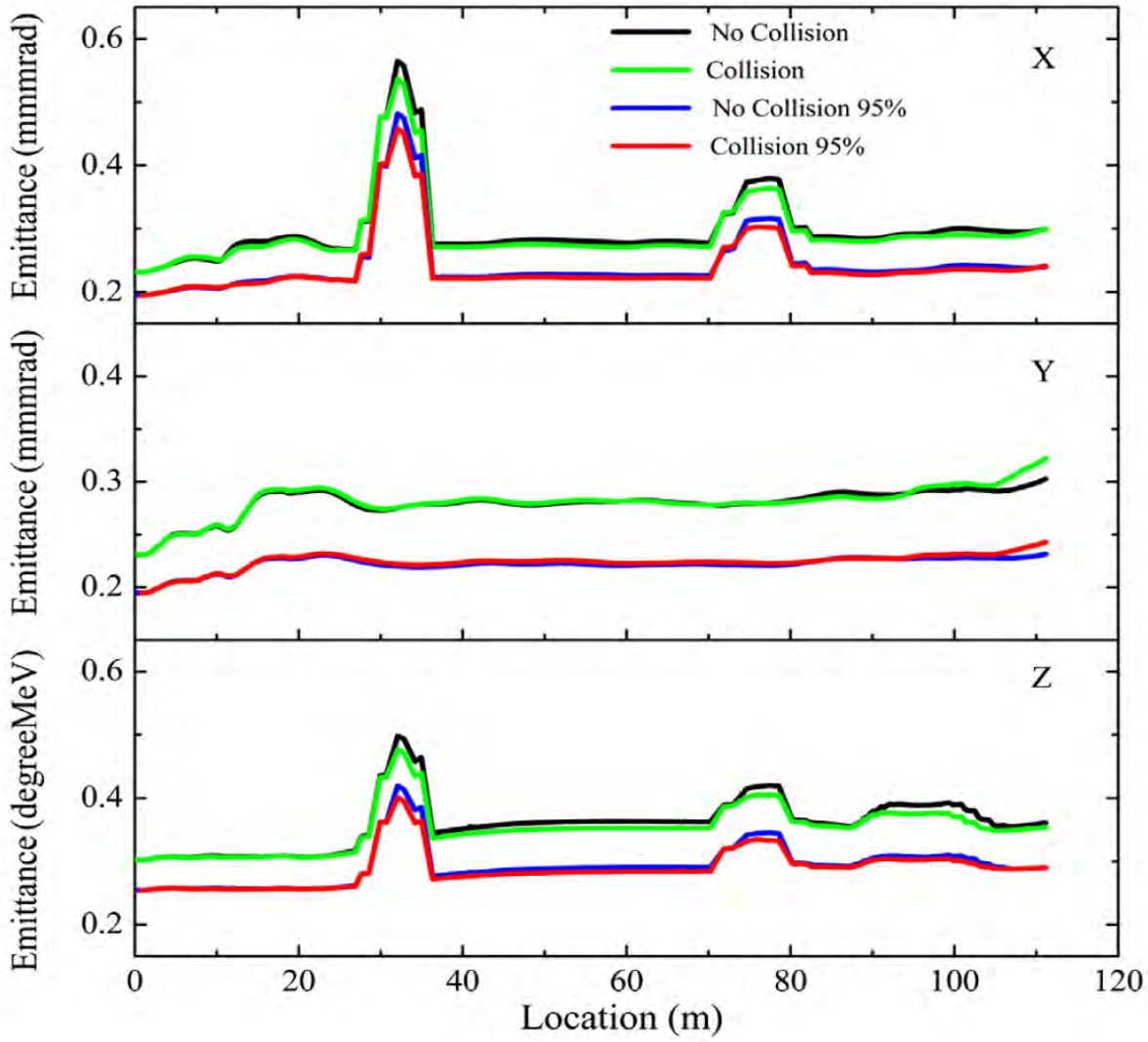

Similar Phase Space Distributions at the Exit of the Linac w/o Collisions

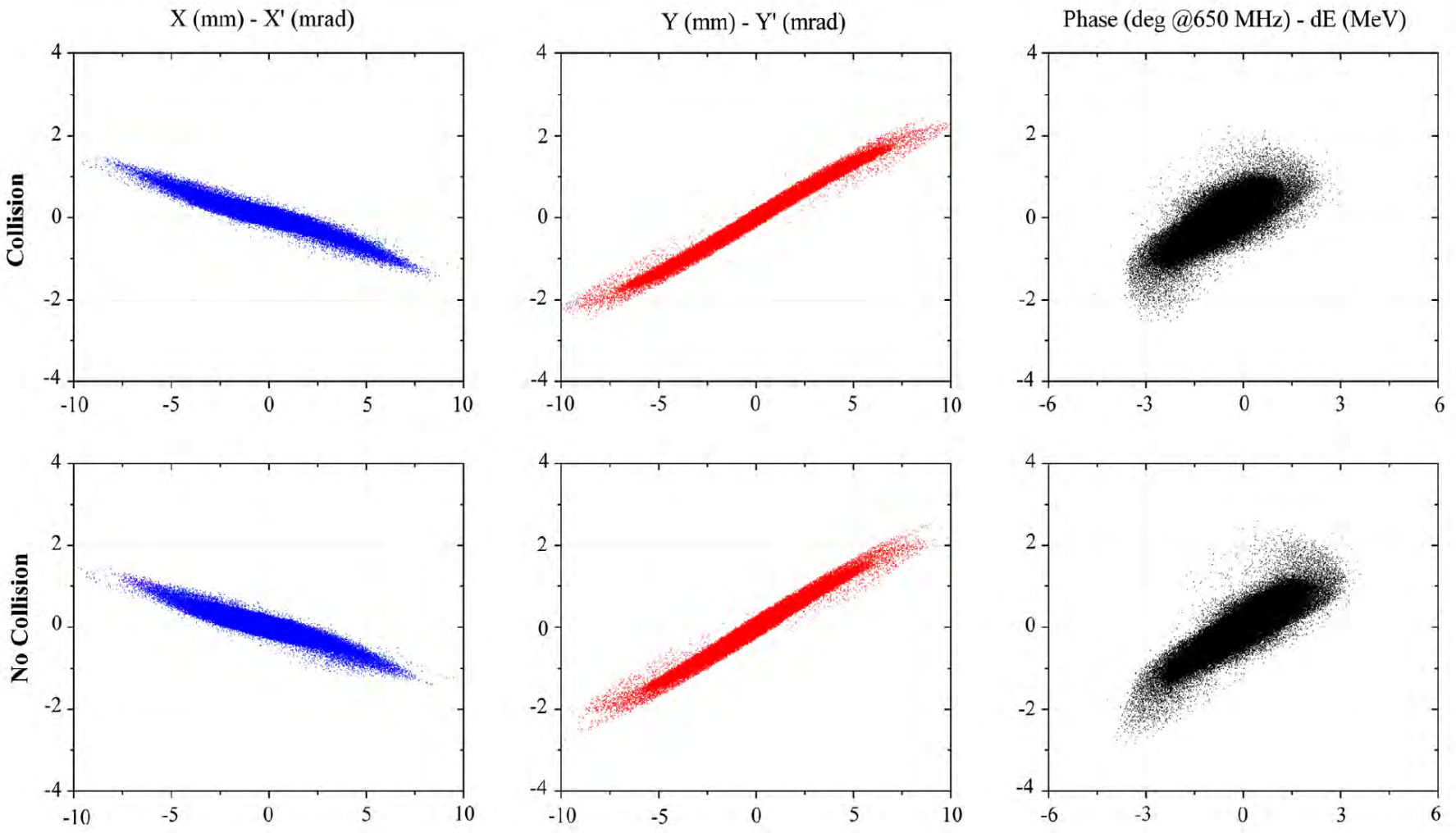

less than 20% differences in all Twiss parameters

Phase Shifter Can be Used for Multiple Proton Beam Passes

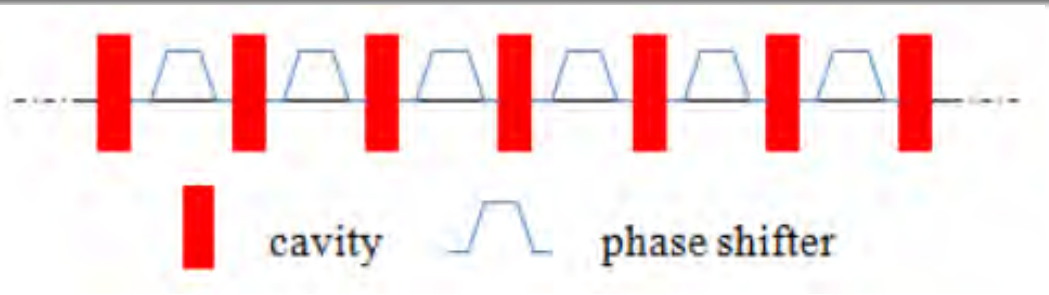

Parameters:

B, E, l_1, l_2

$$P = BR$$

$$R = l_1 / \sin\alpha = P / B$$

$$\alpha = \arcsin(\frac{Bl_1}{P})$$

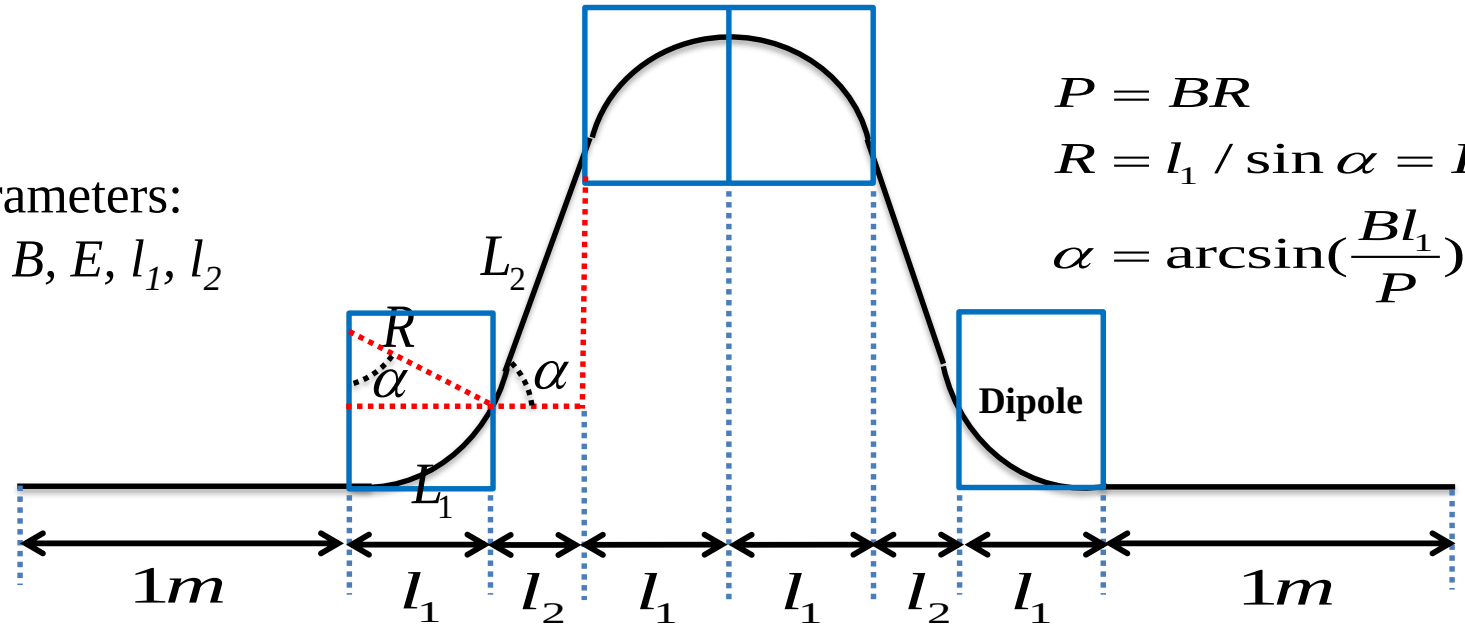

$$\text{path} = 2 + 4\arcsin(\frac{B l_1}{P}) \cdot \frac{P}{B} + 2\frac{l_2}{\sqrt{1-(B l_1 / P)^2}}$$

Fixed Field Phase Shifters for Multi-Pass Proton Linac

- **Phase shifting and focusing requires optimization of a non-linear field profile within the magnet across multiple energies**

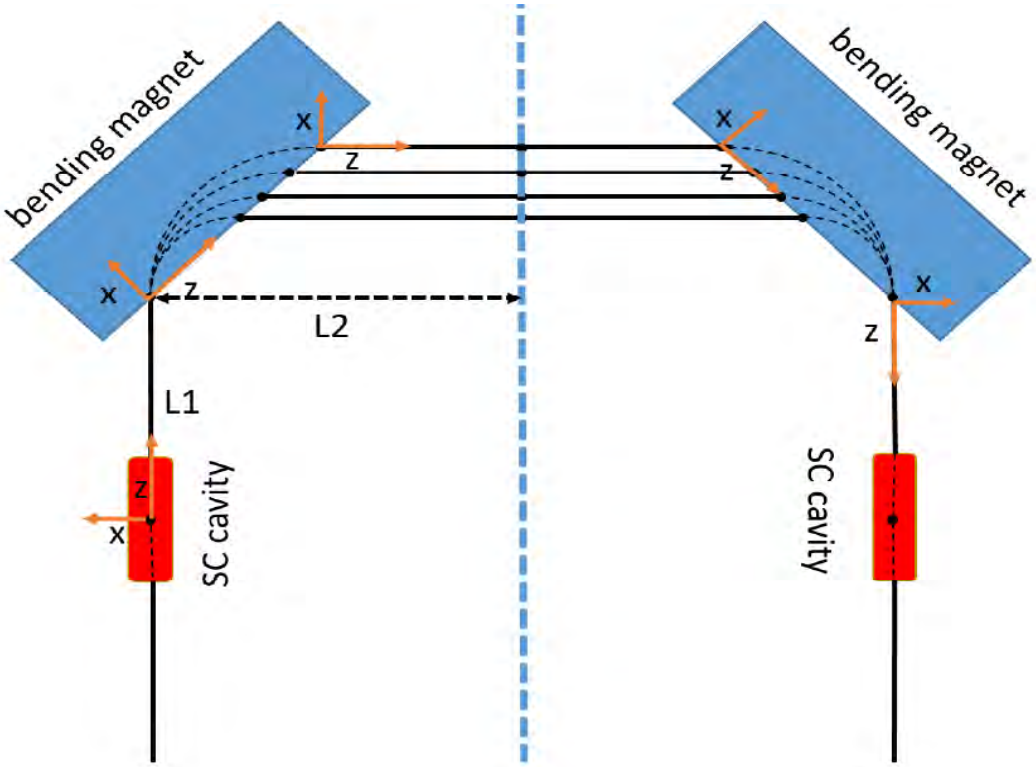

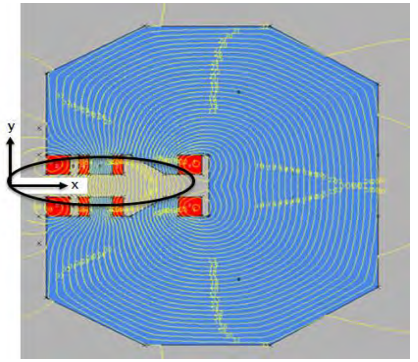

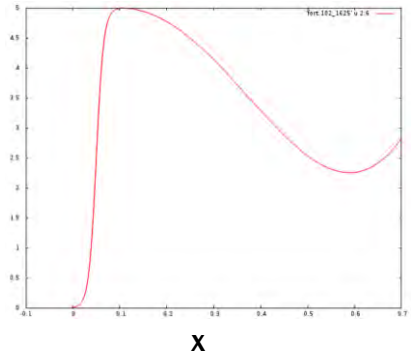

J. Qiang, L. Brouwer, and R. Teyber, Phys. Rev. Accel. Beams **24**, 030101 (2021).

Middle Plane Vertical Magnetic Field Is Approximated Using Multiple Gaussian Wavelets

$$B_y(x) = \sum_{i=1}^{N} a_i \exp\left(-\frac{(x-b_i)^2}{c_i^2}\right)$$

- off-middle plane magnetic fields approximated up to 4th order:

$$B_x(x,y) = y\frac{dB_y(x)}{dx} - \frac{y^3}{6}\frac{d^3B_y(x)}{dx^3}$$

$$B_y(x,y) = B_y(x) - \frac{y^2}{2}\frac{d^2B_y(x)}{dx^2} + \frac{y^4}{24}\frac{d^4B_y(x)}{dx^4}$$

$$B_z(x,y) = 0$$

A Leap-Frog Like Method to Track Middle Plane Particle

$$\frac{d\mathbf{r}}{dt} = \mathbf{v}$$

$$\frac{d\mathbf{v}}{dt} = q\frac{\mathbf{v}}{m\gamma} \times \mathbf{B}$$

$$x = x + \frac{1}{2}\tau v_x$$

$$z = z + \frac{1}{2}\tau v_z$$

$$v_x = v_x - \frac{q}{m\gamma}\tau v_z B_y(x)$$

$$v_z = \sqrt{(c^2 - c^2/\gamma^2 - v_x^2)}$$

$$x = x + \frac{1}{2}\tau v_x$$

$$z = z + \frac{1}{2}\tau v_z$$

$$t = t + \tau.$$

- Energy conservation is guaranteed in this algorithm

Calculation of Transfer Map Using Truncated Power Series Algebra

- Proton beam RMS size evolution using a linear transfer map

$$\Sigma_2 = R\Sigma_1 R^T$$

$$\frac{d\zeta}{ds} = -[H,\zeta]$$

$$\zeta_s = f(\zeta_0) = \sum_i^N \mathrm{M}_i \zeta_0^{\,i}$$

- f can be a very complicated function
- M_i is the i^{th} order transfer map, and is related to the i^{th} derivative of function f

How to attain M_i effectively?

Consider a one-dimensional Taylor approximation:

$$f(x) = f(x_0) + (x-x_0) f'(x_0) + \frac{1}{2!}(x-x_0)^2 f''(x_0) + \frac{1}{3!}(x-x_0)^3 f'''(x_0) + \cdots + \frac{1}{N!}(x-x_0)^N f^{(N)}(x_0)$$

To find the derivative, i.e. Taylor map, one can approximate the derivative numerically:

$$f'(x_0) \approx \frac{f(x_0+\varepsilon) - f(x_0)}{\varepsilon}$$

$$f''(x_0) \approx \frac{f(x_0+\varepsilon) - 2f(x_0) + f(x_0-\varepsilon)}{\varepsilon^2}$$

⇒ loss of accuracy

Introduction to Truncated Power Series Algebra (TPSA)

Use symbolic calculation from package like Mathematica:

For example: $f(x)=\frac{1}{1+x+x^2}$ $f'(x)=\frac{-(1+2x)}{(1+x+x^2)^2}$ $f''(x)=\frac{6x+6x^2}{(1+x+x^2)^3}$

- very complicated for high order derivatives
- even impossible for some function without closed form (e.g. simulation)

Define a N-dimension function space with bases:

$$\{1,(x-x_0),\frac{1}{2!}(x-x_0)^2,\frac{1}{3!}(x-x_0)^3,\cdots,\frac{1}{N!}(x-x_0)^N\}$$

The derivative up to Nth order can be regarded as a point in that space and represented as a vector:

$$Df_{x_0}=[f(x_0),f'(x_0),f''(x_0),f'''(x_0),\cdots,f^{(N)}(x_0)]$$

For example, a constant c, its representation as $Dc=[c,0,0,0,\cdots,0]$

a variable x as, $Dx=[x,1,0,0,\cdots,0]$

$x \Rightarrow y=f(x)$

A point x in number space maps to another point y=f(x) in number space

$Dx \Rightarrow Df_x=f(Dx)$

A point Dx in DA vector space maps to another point Df_x in DA vector space

Basic Operations for the TPSA vector

- A complicated function can be broken down as the operations of **addition** and **multiplication**

  - Rule of addition:

$$Df_{x_0} = [f(x_0), f'(x_0), f''(x_0), f'''(x_0), \cdots, f^{(N)}(x_0)] = [a_0, a_1, a_2, a_3, \cdots a_N]$$

$$Df_{x_1} = [f(x_1), f'(x_1), f''(x_1), f'''(x_1), \cdots, f^{(N)}(x_1)] = [b_0, b_1, b_2, b_3, \cdots b_N]$$

$$Df_{x_0} + Df_{x_1} = [f(x_0) + f(x_1), f'(x_0) + f'(x_1), f''(x_0) + f''(x_1), f'''(x_0) + f'''(x_1), \cdots, f^{(N)}(x_0) + f^{(N)}(x_1)]$$

$$Df_{x_0} + Df_{x_1} = [a_0 + b_0, a_1 + b_1, a_2 + b_2, a_3 + b_3, \cdots, a_N + b_N]$$

  - Rule of multiplication:

$$Df_{x_0} \times Df_{x_1} = ?$$

$$Df_{x_0} \times Df_{x_1} \neq [f(x_0) \times f(x_1), f'(x_0) \times f'(x_1), f''(x_0) \times f''(x_1), f'''(x_0) \times f'''(x_1), \cdots, f^{(N)}(x_0) \times f^{(N)}(x_1)]$$

Basic Operations for the TPSA vector

- Rule of multiplication:

$$(g(x)\times h(x))' = g(x)h'(x) + g'(x)h(x)$$
$$(g(x)\times h(x))'' = g(x)h''(x) + 2g'(x)h'(x) + g''(x)h(x)$$
$$\cdots$$
$$(g(x)\times h(x))^{(N)} = \sum_{k=0}^{N} \frac{N!}{k!(N-k)!} g^{(k)}(x)h^{(N-k)}(x)$$

$$Df_{x_0} \times Df_{x_1} = [f(x_0)f(x_1),\ f(x_0)f'(x_1) + f'(x_0)f(x_1),\ f(x_0)f''(x_1) + 2f'(x_0)f'(x_1) + f''(x_0)f(x_1), \cdots]$$

$$Df_{x_0} \times Df_{x_1} = [a_0b_0, a_0b_1 + a_1b_0, a_0b_2 + 2a_1b_1 + a_2b_0, \cdots, c_N]$$

$$c_N = \sum_{k=0}^{N} \frac{N!}{k!(N-k)!} a_k b_{N-k}$$

- Operation of TPSA/DA vector in a complicated function can be calculated using the rules of addition and multiplication

Example of Calculation of Derivatives Using TPSA

For example, inverse of DA vector $[a_0, a_1, a_2, a_3, \cdots a_N]^{-1} = [x_0, x_1, x_2, x_3, \cdots x_N]$

$$[a_0, a_1, a_2, a_3, \cdots a_N] \times [x_0, x_1, x_2, x_3, \cdots x_N] = [1,0,0,0, \cdots 0]$$

$$[a_0, a_1, a_2, a_3, \cdots a_N]^{-1} = [\frac{1}{a_0}, -\frac{a_1}{a_0^2}, \frac{2a_1^2}{a_0^3} - \frac{a_2}{a_0^2}, \cdots]$$

Another example: evaluate f'(1) and f''(1) for the following function:

$$f(x) = \frac{1}{1+x+x^2}$$

Analytical function method:

$$f'(x) = \frac{-(1+2x)}{(1+x+x^2)^2} \qquad f''(x) = \frac{6x+6x^2}{(1+x+x^2)^3}$$

$$f'(1) = -\frac{1}{3} \qquad f''(1) = \frac{4}{9}$$

TPSA method:

$$x = 1 \qquad D1 = [1,1,0]$$

$$Df_1 = f(D1) = \frac{1}{1+[1,1,0]+[1,1,0]^2} = \frac{1}{[1,0,0]+[1,1,0]+[1,2,2]} = \frac{1}{[3,3,2]} = [\frac{1}{3}, -\frac{3}{9}, \frac{18-6}{27}] = [\frac{1}{3}, -\frac{1}{3}, \frac{4}{9}]$$

Numerical Tracking of a DA/TPSA Particle

A DA/TPSA particle

$$(X, V_x, Y, V_y, T, V_z)$$

$$\frac{d\mathbf{r}}{dt} = \mathbf{v}$$

$$\frac{d\mathbf{v}}{dt} = q\frac{\mathbf{v}}{m\gamma} \times \mathbf{B}$$

$$X = X + \frac{1}{2}\tau_z \frac{V_x}{V_z}$$

$$Y = Y + \frac{1}{2}\tau_z \frac{V_y}{V_z}$$

$$T = T + \frac{1}{2}\tau_z \frac{1}{V_z}$$

$$z = z + \frac{1}{2}\tau_z$$

$$c^2\beta^2 = V_x^2 + V_y^2 + V_z^2$$

$$V_x = V_x - \frac{q}{m\gamma}\tau_z B_y(X, Y)$$

$$V_y = V_y + \frac{q}{m\gamma}\tau_z B_x(X, Y)$$

$$V_z = \sqrt{c^2\beta^2 - V_x^2 - V_y^2}$$

$$X = X + \frac{1}{2}\tau_z \frac{V_x}{V_z}$$

$$Y = Y + \frac{1}{2}\tau_z \frac{V_y}{V_z}$$

$$T = T + \frac{1}{2}\tau_z \frac{1}{V_z}$$

$$z = z + \frac{1}{2}\tau_z.$$

An Application of Multi-Pass Recirculating Superconducting Proton Linac

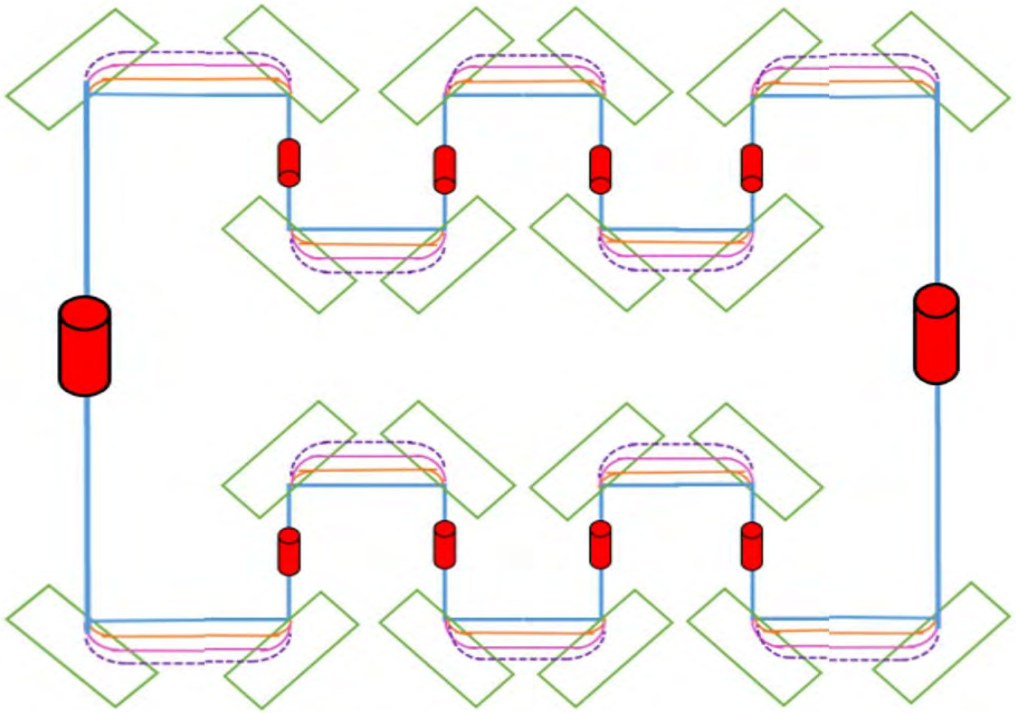

- Energy from 150MeV to 600MeV
- 10 superconducting cavities
- Four passes, 112.5 MeV average energy gain per pass

Proton Beam Horizontal Centroid Evolution through an Entrance Phase Shifter

horizontal centroid evolution with different energies

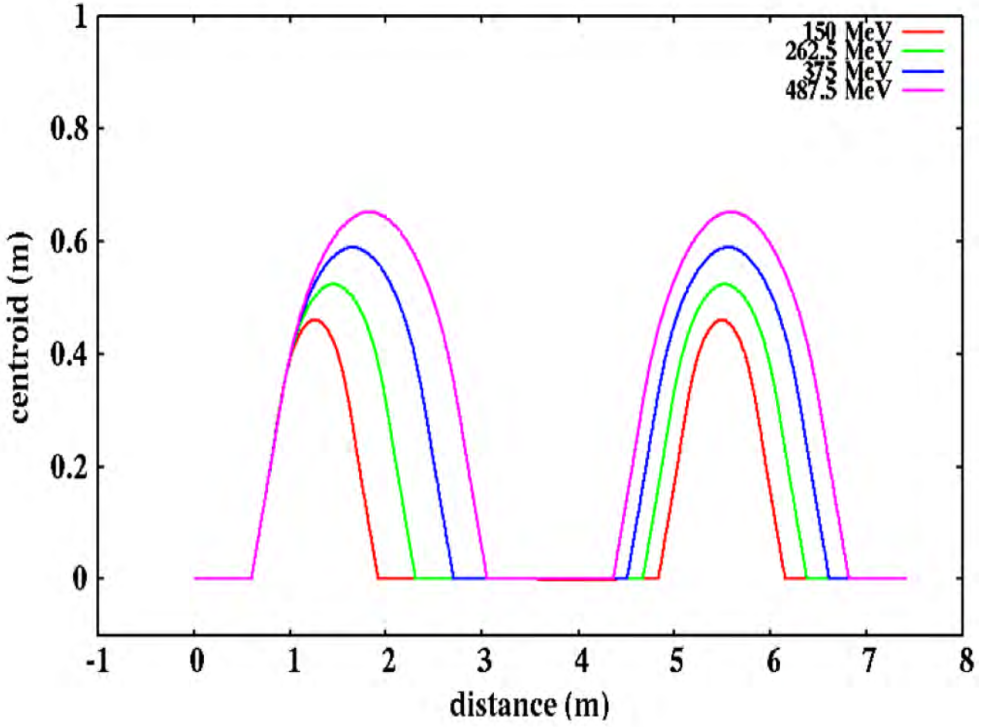

middle plane vertical B field

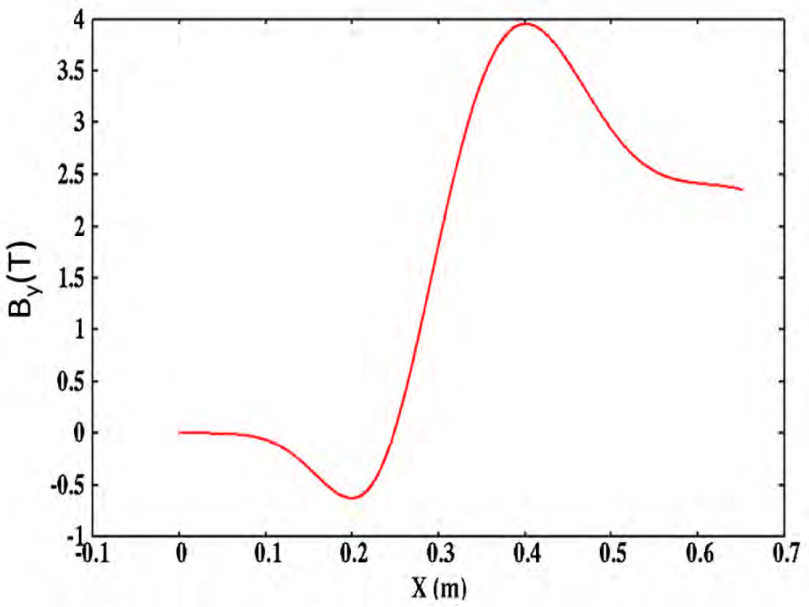

- Vertical B field is optimized to meet longitudinal synchronous conditions and beam size constraints with multiple energies.

Proton Beam Transverse and Longitudinal RMS Emittance Evolution through an Entrance Phase Shifter (40 mA current)

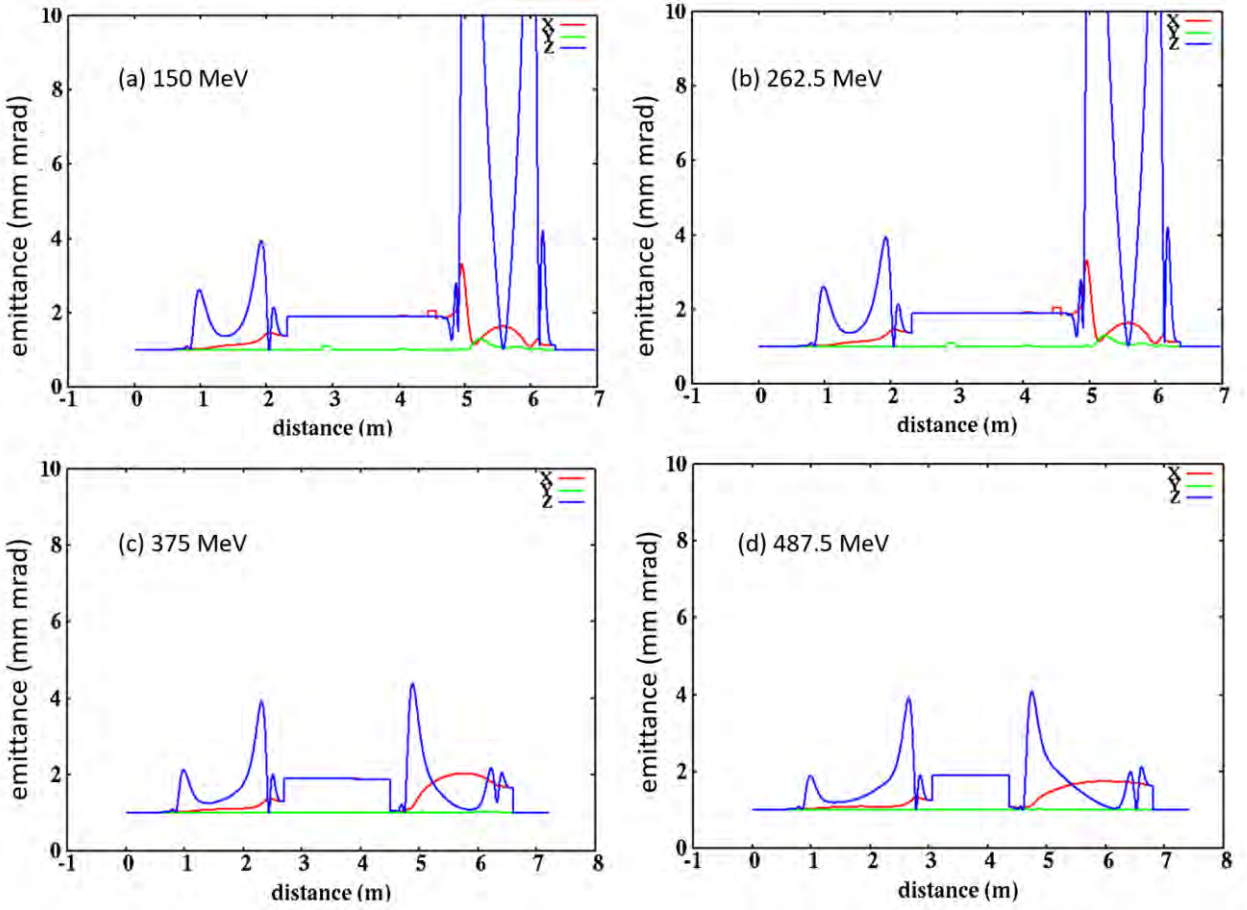

- Initial emittances can be preserved through the phase shifter after optimization

Proton Beam Transverse and Longitudinal RMS Size Evolution through an Entrance Phase Shifter (40 mA current)

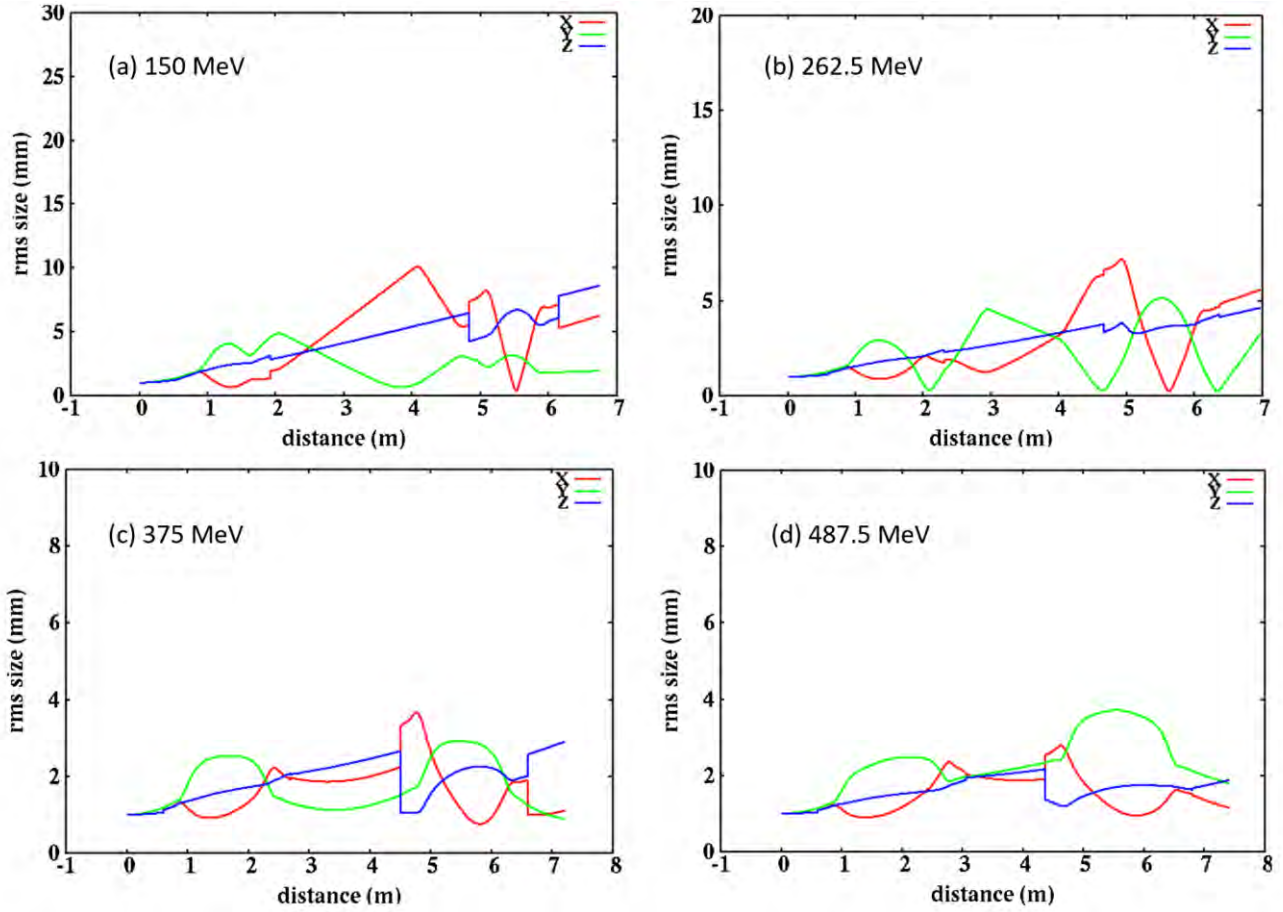

- Proton beam sizes can be controlled with reasonable sizes after optimization

Proton Beam Transverse and Longitudinal RMS Emittance Evolution through an Exit Phase Shifter (40mA current)

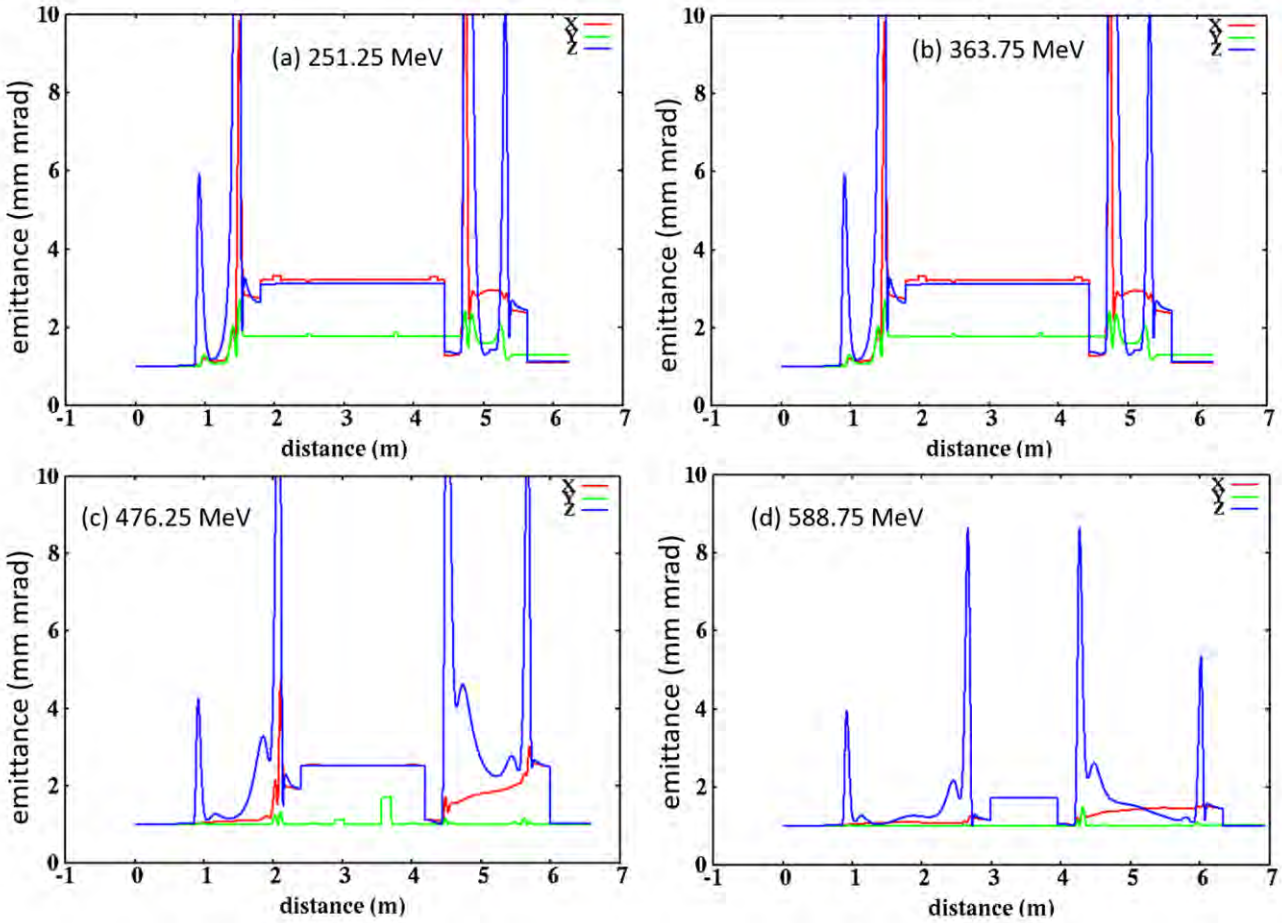

- Emittances can be preserved through the phase shifter after optimization

Proton Beam Transverse and Longitudinal RMS Size Evolution through an Exit Phase Shifter (40 mA current)

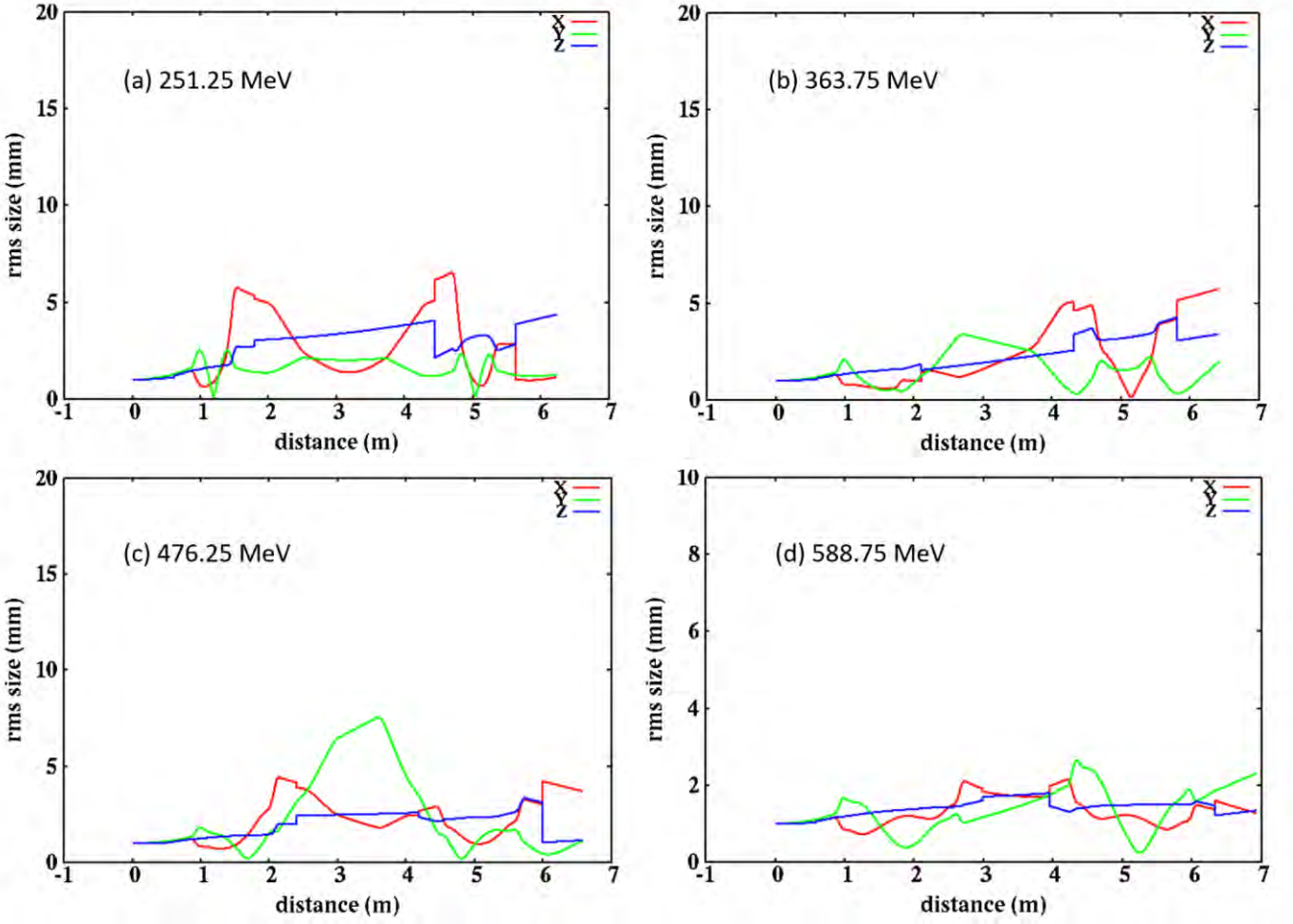

- Proton beam sizes can be controlled with reasonable sizes after optimization

Future Work

- Start-to-end beam dynamics design of a multi-pass recirculating proton linac
- Study of the proton injection and extraction
- Study of the effects of machine imperfections and RF cavity failure
- Engineering design of bending magnets
- Experimental demonstration of a recirculating proton linac
- ....

Acknowledgements

- We would like to thank Drs. L. Brouwer, R. Teyber, K. Hwang and Y. Tao for the collaboration, and Drs. Z. Liu and Y. Hao for the TPSA library used in this study.

- This work was supported by the U.S. Department of Energy under Contract no. DE-AC02-05CH11231 and used computational resources at National Energy Research Scientific Computing Center (NERSC).

Thank You!

Backup Slides

Global Optimization Using a Stochastic Evolutionary Method to Overcome Local Optimal Solution

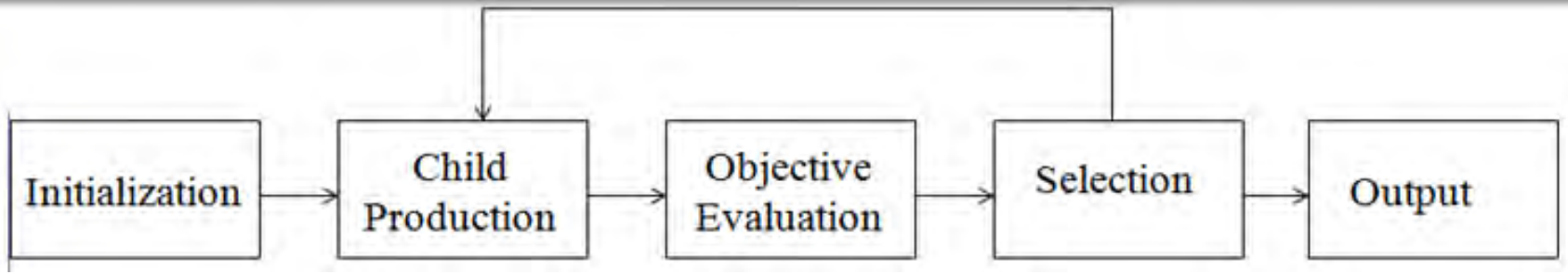

Differential Evolution Algorithm:

- Stochastic, population-based evolutionary optimization algorithm
- Easy to implement and to extend to multi-processor
- DE has been shown to be effective on a large range of classic optimization problems
  - In a comparison by Storn and Price in 1997 DE was more efficient than simulated annealing and genetic algorithms
  - Ali and Torn (2004) found that DE was both more accurate and more efficient than controlled random search
  - In 2004 Lampinen and Storn demonstrated that DE was more accurate than several other optimization methods including four genetic algorithms, simulated annealing and evolutionary programming

R. Storn and K. Price, Journal of Global Optimization 1a1:341-359, (1997).

Differential Evolution Algorithm

- A population of control parameter vectors are randomly generated from the control parameter space
- A new perturbed vector is generated for each parent by:

$$v_i = x_{i,G} + \lambda (x_{best,G} - x_{i,G}) + F(x_{r2,G} - x_{r3,G})$$ → *mutation*

- A new trial control parameter vector is generated by:

$$U_{i,G+1} = (u_{i1,G+1}, u_{i2,G+1}, \cdots, u_{iD,G+1})$$

$$u_{ij,G+1} = \begin{cases} v_{ij}, \text{ if } rand_j \le CR \text{ or } j = mbr_i \\ x_{ij}, \text{ otherwise} \end{cases}$$ → *cross over*

- If the new trial vector produces a better objective function value, it will be put into the next generation *G+1* population. Otherwise, the original parent vector is kept in the next generation population.

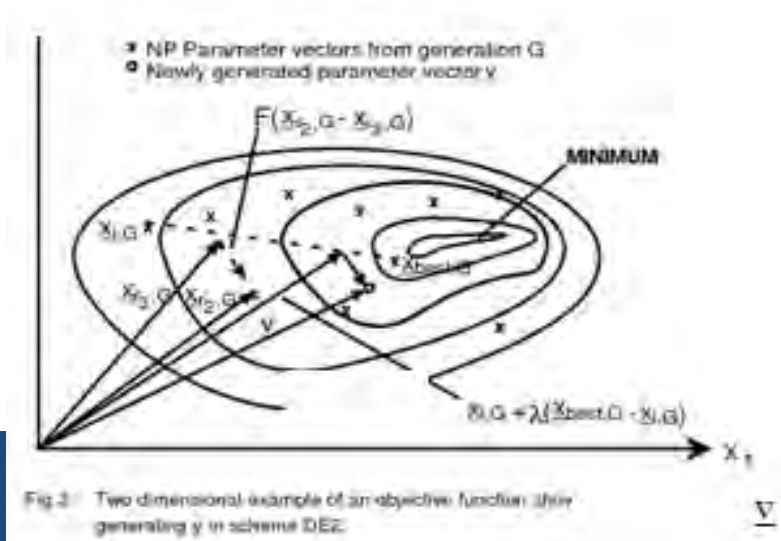

Fig.2 Two dimensional example of an objective function showing generating y in scheme DE2.

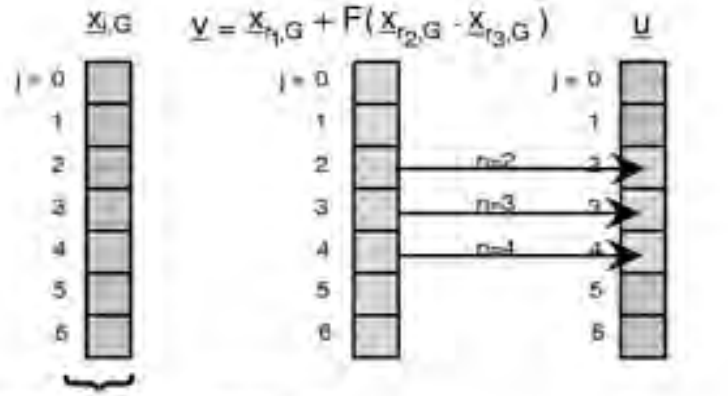

...stration of the crossover process for D=7, n=2 and L=3.

An Adaptive Unified Differential Evolution Algorithm:
Reduce the Number of Mutation Strategies

Some standard DE mutation strategies:

DE/rand/1: $\vec{v}_i = \vec{x}_{r1} + F_{xc}(\vec{x}_{r2} - \vec{x}_{r3})$

DE/rand/2: $\vec{v}_i = \vec{x}_{r1} + F_{xc}(\vec{x}_{r2} - \vec{x}_{r3}) + F_{xc}(\vec{x}_{r4} - \vec{x}_{r5})$

DE/current-to-best/1: $\vec{v}_i = \vec{x}_i + F_{cr}(\vec{x}_b - \vec{x}_i) + F_{xc}(\vec{x}_{r1} - \vec{x}_{r2})$

DE/current-to-rand/1: $\vec{v}_i = \vec{x}_i + F_{cr}(\vec{x}_{r1} - \vec{x}_i) + F_{xc}(\vec{x}_{r2} - \vec{x}_{r3})$

DE/rand-to-best/1: $\vec{v}_i = \vec{x}_i + F_{cr}(\vec{x}_b - \vec{x}_i) + F_{xc}(\vec{x}_{r2} - \vec{x}_{r3})$

. . .

randomly chosen solutions

current solution

best solution

Unified DE mutation strategy (uDE):

$$\vec{v}_i = \vec{x}_i + F_1(\vec{x}_b - \vec{x}_i) + F_2(\vec{x}_{r1} - \vec{x}_i) + F_3(\vec{x}_{r2} - \vec{x}_{r3})$$

Encompasses standard DE mutation strategies as special cases. Four control parameters + CR

$$F_{j,i}^{G+1} = \begin{cases} F_{jmin} + r_{j1}(F_{jmax} - F_{jmin}), & \text{if } r_{j2} < \tau_j \\ F_{j,i}^{G}, & \text{otherwise} \end{cases}$$

J. Qiang et al., in Proc. CEC2016, Vancouver (IEEE, Piscataway, NJ, 2016), p. 4061.